CHAPTER VI

THERMAL, CRYSTALLIZATION, MECHANICAL, AND RHEOLOGICAL CHARACTERISTICS OF POLY(TRIMETHYLENE TEREPHTHALATE) /POLY(ETHYLENE TEREPHTHALATE) BLENDS

Nujalee Dangseeyun, Pitt Supaphol*, and Manit Nithithanakol

The Petroleum and Petrochemical College, Chulalongkorn University, Soi Chula12, Phyathai Road, Pathumwan, Bangkok 10330, THAILAND

ABSTRACT

Blends of PTT and PET exhibited single glass transition temperatures at all compositions studied, suggesting miscibility of the two components in the amorphous phase. The crystallization peak temperature from the glassy state for these blends was found to increase with increasing PTT content, possibly as a result of increased mobility of the blend. The results from crystallization from the melt suggested that the crystallization process was retarded due to the presence of the minor phase in the blend, possibly as a result of decreased diffusional mobility. Observation of the subsequent melting behavior (after crystallization from the glassy state) and X-ray diffractograms suggested that, upon crystallization, PTT and PET were phase-separated. As increase in minor phase composition caused a lowering in the apparent melting temperature. The apparent degree of crystallinity for each component was found to decrease with increasing minor component, with a 50:50 w/w blend of PTT and PET exhibiting the lowest total crystallinity and the lowest tensile strength, suggesting that this composition showed the most phase-separation. The results from dynamic rheological measurements showed that these blends exhibited a negative deviation from the log-additivity rule, inferring that these blends were miscible in the melt state.

(**Key-words**: poly(ethylene terephthalate); poly(trimethylene terephthalate); blends)

---

*To whom correspondence should be addressed: Fax: +66-2215-4459; E-mail address: pitt.s@chula.ac.th

1. INTRODUCTION

Poly(trimethylene terephthalate) (PTT) is a novel linear aromatic polyester, that was successfully synthesized by Whinfield and Dickson in 1941[1], but it was not commercial produced because of the lack of an economical source of 1,3-propanediol which is one of the raw materials used to produce PTT. Nevertheless, the synthesis of PTT is now commercially available and has been produced by Shell Chemicals company under the tradename Corterra, joining the rank of other linear aromatic polyesters, poly(ethylene terephthalate) (PET) and poly(buthylene terephthalate) (PBT). PTT has properties immediately between those of PET and PBT with an unusual combination of the outstanding properties of PET and processing characteristics of PBT.

The miscibility and the crystallization behavior of polymer blends have been widely and intensively studied. There are many researches carried out on blending of polyesters such as PET/PBT blends [2-9], PET/PC blends [10,11] and PET/PEI blends [12,13]. However in the case of PTT, that is one of aromatic polyesters, there is a few research [14] studied on blending with other polymers. Therefore this work is aimed at studying the miscibility, melting, crystallization behavior, mechanical property and also processability of PTT/PET blends.

The study on miscibility of PET/PBT blends were carried out by many researchers. Escala and Stein [2] found that the blends were compatible in amorphous phase and showed a single glass transition temperature varied with composition. The similar result was predicted by Mishra and Depura [3] and also reported by Avramova [6], Shonaike [7]. The crystallization behavior of PET/PBT blends was studied by using X-ray, DSC and IR [2]. The results showed that these blends crystallized into separated crystals of the two components rather than co-crystallization. Avramova [6] also reported the same result that each component formed its own crystal phase and the presence of the other component did not disturbed and even enhanced the crystallization process.

For thermoplastic polyesters, a transesterification reaction is commonly occurred when they processed near or above their melting temperatures, resulting in deterioration of mechanical properties, and/or a decrease in molecular weight. In

PET/PBT blends, Escala and Stein [2] found that no transesterification occurred during preparation of the melted-samples within at least three minutes. However the crystallization behavior from glassy state were influenced by entanglement and tranesterification of chain [8]. Lee *et al.* [9] found that the modified surface of $BaSO_4$ with a coupling agent can be suppressed the transesterification of PTT/PBT blends [9]. The formation of the block copolymer-like structure for the polyester stuck to the $BaSO_4$ particle facilitated crystallization by providing a crystallization nucleus without significant transesterification reaction, resulting in higher mechanical properties.

Recently, Huang and Chang [14] observed a single and composition-dependent glass transition temperatures over the entire composition range of PTT blended with poly(ether imide) (PEI). This implies that these blends were fully miscible in amorphous region. Moreover, the presence of PEI content in the blends retards or inhibits PTT segments migrated to the crystallite-melt interface lead to the prevention of PTT to recrystallize during heating scan in DSC.

2. EXPERIMENTAL DETAILS

2.1. Materials

PTT was obtained from Shell Chemical Company (USA) Ltd. in the pellet form (CP509201 grade). The number and weight average molecular weights determined by gel permeation chromatography (GPC) were 25840 and 47680 g mol^{-1}, respectively. The molecular weight distribution was 2.25. PET used in this study was a commercial product from Indo PET (Thailand) Ltd. in the form of pellets (N1 grade, M_n = 34030, M_w = 59140, PD = 2.05).

2.2. Sample Preparation

The pellets of PTT and PET were dried in a vacuum oven at 140°C for 5 hours and then were premixed in a dry mixer. A series of PTT/PET blends were prepared at ratio of 0/100, 10/90, 25/75, 40/60, 50/50, 60/40, 75/25, 90/10, and 100/0, and were then melt-blended using a Collin co-rotating twin screw kneader ZK 25 (25mm x 30D) at 280°C with the screw speed of 70 rpm. After that each blend was melted-pressed at 280°C in a Wabash V50H compression molding machine

under a pressure of 4.62×10^2 MNm^{-2} for 5 minutes, and then cooled down to 40°C under pressure. The samples were cut into films and specimen for each test. This treatment assumes that previous thermo-mechanical history was essentially erased, and provided a standard crystalline memory condition for the as-prepared film.

2.3. Differential Scanning Calorimetry Measurements

The thermal properties of these PTT, PET, and blends were investigated using a Perkin-Elmer Series7 Differential Scanning Calorimetry (DSC-7). Calibration for temperature scale was carried out using a pure indium standard (T^0_m = 156.6 °C and ΔH^0_f = 28.5 J g^{-1}) on every other run to ensure accuracy and reliability of the data obtained. To minimize thermal lag between polymer sample and DSC furnace, each sample holder was loaded which weighed around 8.0 ± 0.5 mg. It is worth noting that each sample was used only once and all the runs were carried out under nitrogen atmosphere to prevent extensive thermal degradation. For the glass transition temperature (T_g) measurement, the samples were heated from 40°C at a heating rate 80°C min^{-1} to a fusion temperature T_f of 280°C, and then kept at this temperature for 5 minutes in order to erase the previous thermal histories. After that each sample was immediately quenched in liquid nitrogen. Upon re-heating at 10°C min^{-1} from 25 to 280°C, a glass transition temperature (T_g) was observed as an inflection point. Finally, the sample was cooled from 280 to 40°C at a heating rate of 10°C min^{-1}, in order to observe the crystallization temperature from the melt state (T_c).

2.4. Thermogravimetric Analysis

In order to obtain the decomposition temperature of pure polymers and its blends, the TGA measurement were performed on a DuPont Instrument model 2950 by heating from 30 to 700°C with a heating rate of 10°C min^{-1} under a nitrogen atmosphere. The 10% weight loss temperature (T_{onset}) and the 50% weight loss temperature (T_{50}) were obtained on the heating scans.

2.5. Crystal Structure and Crystallinity

Wide-angle X-ray diffraction (WAXD) technique was employed to determine crystal modification and apparent degree of crystallinity of pure polymers and its blends prepared at the same condition (i.e., nonisothermal crystallization condition at cooling rate of $10^{o}C\ min^{-1}$) set forth for samples prepared for the DSC measurements. Each sample was then taken out of the DSC sample holder and was then pasted onto a glass X-ray sample holder, using Vaseline as adhesive. The WAXD intensity pattern of each sample was then collected on a Rigaku Rint 2000 diffractometer, equipped with a computerized data collection and analytical tools. The X-ray source (CuKα radiation, λ = 1.54 Å) was generated with an applied voltage of 40 kV and a filament current of 30 mA.

2.6. Mechanical Property

Tensile strength of PTT, PET, and blends were determined using an Instron Universal Testing Machine Model 4206 according to ASTM D638-91 test method. The tests were carried out using a 100 kN load cell at and 5 mm min^{-1} cross-head speed. Dumbbell shape specimens were cut from the as-prepared sheets using a plastic sample cutting machine, and the specimen dimensions, were as follow: width of narrow section was 13 mm and the gauge length was 50 mm. The results were obtained from a mean value of five specimens.

2.7. Cone and Plate Rheometer

Steady and dynamic shear rheological measurements were carried out on ARES Rheometric Scientific with cone-and-plate geometry. Pellets of the blends were compressed into circular disk of 1 mm thickness and 25 mm diameter. Before the measurement was taken, the rheometer was heated up to 260°C, and the gap was set to 0.052 mm. For the steady rate sweep test, shear viscosity was determined as a function of shear rate. In case of.dynamic measurements, the strain (γ) values were chosen in order to perform the experiments in the linear viscoelastic region i.e., the limiting strain under which the rheological parameters (G', G'', η^*, etc.) remained constant.

3. RESULTS AND DISCUSSION

3.1. Thermal Stability

Thermogravimetric analysis is the most popular method used to characterize thermal stability of polymers. PTT and PET are the member of the thermally stable polymers, they show the well thermal stability below 300°C, therefore, it should be noted that there is no decomposition occur in the DSC and rheological testing experiment. PTT starts to decompose at around 375°C, whereas PET, that has higher thermal stability, begins to decompose at around 410°C. The completely decomposition temperature of PTT and PET appear at around 520 and 620°C, respectively, Figure 1 illustrates the plots of the 10% weight loss temperature (T_{onset}) and the 50% weight loss temperature (T_{50}) decrease with PTT content in the blends. It is obvious that, the T_{onset} and T_{50} of these blends decrease with increasing PTT content, implying that the thermal stability of these blends decrease with increasing PTT content. In the other words, the thermal stability of PTT can be improved by blending with PET.

3.2. Miscibility of PTT/PET blends

Differential scanning calorimetry is the most widely method that used to investigate the miscibility in polymer blends. Figure 2a and 2b show the DSC heating thermogram (10°C min^{-1}) for quenched PTT/PET blends and the DSC crystallization exotherms from melting state of PTT/PET blends, respectively. Based on the plot shown in Figure 2a, it can be observed that each blend composition showed only one single glass-transition temperature appear at the intermediate temperature between those of pure polymers. The glass-transition temperature of each blend decreases with increasing PTT content. From these results, it can be indicated that these blends are fully miscible in amorphous phase. For a miscible polymer blends, there are several equations used to predict the T_g-composition dependence of the blends, as those proposed by Couchman-Karasz [15], Gordon-Taylor [16], Utracki [17], and Fox [18]. These equations, with different approximations, predict a monotonic dependence of T_g upon composition, and do not

give any cusp in the predicted curve. However one of the most used expressions of T_g-composition dependence of miscible polymer blends is the Fox's equation [18].

$$\frac{1}{T_g} = \frac{W_1}{T_{g1}} + \frac{W_2}{T_{g2}} \quad (1)$$

Where W_1 and W_2 are the weight fractions of components 1 and 2, respectively (in the amorphous phase), and T_{g1} and T_{g2} are the respective T_{gs} of the pure components. Equation 1 (Fox's equation) assumes random mixing between the blend components, equal values of the differences between specific heats of the liquid and the glassy states in the glass transition range of the two components (i.e., $\Delta C_{p1} = \Delta C_{p2}$), and no volume expansion between the two components during mixing. Figure 3 shows the predicted curve of PTT/PET blends by the Fox equation using T_g (PTT) = 43.1°C and T_g (PET) = 76.6°C. It is apparent that the measured T_g of the blends does not fit well with the predicted T_g value from the Fox equation. Another one of the most used equations of T_g-composition dependence of miscible blends is the Gordon-Taylor's equation [16].

$$T_g = \frac{W_1 T_{g1}}{W_1} + \frac{kW_2 T_{g2}}{kW_2} \quad (2)$$

Where k is the adjustable parameter, and k = 0.96 suitable for this system. The predicted T_g value from the Gordon-Taylor's equation is shown as solid line in Figure 3. On the contrary to the Fox equation, the Gordon-Taylor's equation [16] provides a satisfactory description for the T_g-composition relationship.

3.3. Crystallization Behavior

The plots of the cold crystallization temperature (T_{cc}) and the crystallization temperature from melting state (T_c) of the blends against PTT content are shown in Figure 4 and 5, respectively. The T_{cc} and T_c of PTT are 68.8 and 179.8°C, respectively and that for PET are 139.4 and 190.3°C, respectively. The cold crystallization temperature (T_{cc}) of the blend tends to decrease with increasing PTT content, implying that the crystallization rate of the blend increases with increasing PTT content. This can be explained by the faster crystallization rate of PTT when compare to that of PET. Hence the presence PTT will improve or enhance the crystallization rate from glassy state of the blends. However the crystallization

temperature from melting state (T_c) was found to decrease as increasing the second component in the blend. It can be indicated that the minor component in the blends retards or inhibits the major component to crystallize from the melting state, in the other word, the crystallization rate of the major component in the blend decreases with increasing the minor component.

3.4. Melting Behavior

The plots of melting endotherm of PTT, PET, and blends with PTT content are shown in Figure 6. It can be observed that the melting temperature (T_m) of PET and PTT are ca. 247.0, 226.8°C, respectively. At 10% PTT content, the blend shows a single melting endotherm, indicated that the minor component in the blend is not enough to form its own crystal phase, however it is sufficient to affect the glass transition temperature and the crystallization process of the blends. The double melting peaks of PTT/PET blends were observed at 25, 40, 50, and 60% PTT contents with the higher the content of one component in the blends, the higher the corresponding maximum DSC melting peaks were observed. Based on this result, it can be indicated that each component in the blends forms its own crystal phase rather than co-crystallization. This can be confirmed by the presence of the characteristic X-ray peaks of PTT and PET in blends.

According to the plot shown in Figure 2, it is obvious that these PTT/PET blends show the melting point depression, that the melting point of each component in the blends decreased with increasing the content of the other component. The melting point depression can be used to study polymer interactions when one of the polymer components in the blends is partially crystalline. Due to the lower chemical potential in a miscible polymer blend when compare to the pure state, the temperature at which its crystals are in equilibrium with the miscible amorphous phase will be lower, that means, the melting point depression occurs [19]. The melting point depression of both crystalline components, PET/PBT blends, was observed by many researchers [6,20]. They found that the blends were miscible in amorphous state and showed a single glass transition temperature intermediate between those of pure components.

3.5. Crystal Structure and Crystallinity

Wide angle X-ray diffractometer was used to observe the crystal structure and the resulting apparent degree of crystallinity of PTT, PET, and blends. Figure 7 illustrates the WAXD patterns of PTT, PET and blends (each sample was prepared in DSC cell by cooling ($10^{o}C\ min^{-1}$) to 30°C after complete melting at 280°C for 5 min). Table 1 shows the characteristic X-ray peaks of PTT, PET and blends. For pure PTT samples, the characteristic X-ray peaks were observed at the scattering angles 2θ of ca. 15.3, 16.8, 19.4, 21.7, 23.6, 24.6 and 27.3°, corresponding to the reflection planes of $(010),(0\bar{1}2),(012),(10\bar{2}),(102),(1\bar{1}3),(10\bar{4})$, respectively [21]. In case of PET, it shows the characteristic X-ray peaks at the scattering angle 2θ of ca. 16.1, 17.5, 21.6, 22.8, 25.9, 28.1, and 32.6°, corresponding to the reflection planes of $(0\bar{1}1),(010),(\bar{1}11),(1\bar{1}0),(100),(1\bar{1}1),(101)$, respectively [22]. Based on Figure 7, it can be observed that no new peak occurs in diffraction pattern, implying that PTT and PET crystallize separately and there is no co-crystallite in the blends under our experimental condition. Both PTT and PET crystallize into triclinic crystal structure. Desborough et al. [23] determined the unit cell dimensions of PTT from WAXD with axes a = 4.64 A°, b = 6.27 A°, c = 18.64 A°, α = 98°, β = 90°, and γ = 111°. For PET, the axes of crystal structure was found to be a = 4.56 A°, b = 5.94 A°, c = 10.75 A°, α = 98.5°, β = 118°, and γ = 112° [22].

Figure 8 shows the degree of crystallinity of PTT and PET in the blends. By referring to the relative ratio of the integrated intensities under the crystalline peaks A_c to the integrated total intensities A_t (i.e., $A_t = A_c + A_a$, where A_a is the integrated intensities under the amorphous halo)., i.e.,

$$\chi^{WAXD} = \frac{A_c}{A_c + A_a} \in [0,1] \tag{3}$$

It can be seen that the degree of crystallinity of PTT and PET are ca. 24.8 and 22.3%, respectively. Chuah [1] found that PTT tended to crystallize in a melt processes with degree of crystallinity ca. 15 and 30 wt.%. In case of PTT/PET blends, the degree of crystallinity of each component in the blends decreases as increasing the other component. Based on the total degree of crystallinity shown in Table 1, it should be noted that the blend of 50PTT/50PET shows the lowest total degree of crystallinity.

3.6. Mechanical Property

Figure 9 shows tensile strength of PTT, PET and blends according to ASTM D638-91 test method. In our experiment, the tensile strength of PTT was found to be 58.3 MPa, which is quite lower than that reported by Chuah [1]. In case of PET, it was found to be 73.8 MPa, which is comparable to previous reported [1]. Based on the plot shown in Figure 9, it is obvious that pure PET provides the highest tensile strength. In PET-rich blends, the tensile strength was found to increase as increasing PTT content, and for PTT-rich blends, the tensile strength also increases as increasing PET content. The lowest tensile strength was found in 50PTT/50PET blend. This result can be described by the phase separation of two crystalline polymers and the lowest total degree of crystallinity.

3.7. Melt Rheology

Processability of PTT/PET blends can be estimated by measuring their steady-state shear viscosity. Figure 10 shows the steady shear viscosity, η obtained at a temperature 260°C for PTT, PET, and blends as a function of shear rate (s^{-1}). At shear rate studied (0.25 to 25 s^{-1}), it can be observed that the shear viscosity of these blends slightly decrease with increasing shear rate, implying that these blends behave as shear thinning at low shear rate. Chuah [1] found that the melted PTT is nearly Newtonian at low shear rate and it behaves a shear thinning at shear rate greater than 1000 s^{-1}.

Figure 11 illustrates the zero shear viscosity values (viz. taken as the viscosity values at the shear rate of ca. 0.25 s^{-1}) of PTT, PBT and blends. It is obvious that PTT provides the highest zero shear viscosity and it decreases as increasing PTT content. It reaches a minimum at 50% PTT and increases as increasing PTT content. The highest zero shear viscosity of PET can be explained by the highest melting point of PET when compare to the experimental temperature (260°C). The decrease of the zero shear viscosity when increasing PTT content due to the depression of melting temperature of the blends, which can directly affected to the viscosity at 260°C.

The plots of complex viscosity (η^*) at constant frequency with the blend composition are shown in Figure 12. In polymer blends, the composition dependence of viscoelastic functions gives much information about the degree of miscibility of polymer blends, the viscoelastic functions usually follow the log-additivity rule

$$\log F_b = \phi_m \log F_m + \phi_d \log F_d \qquad (4)$$

where F is a viscoelastic function, ϕ is a volume fraction, and subscript "b", "m", and "d" indicate the values for the blend, the matrix, and the dispersed phase, respectively [24]

For immiscible polymer blends, the viscoelastic functions deviated from the log-additivity rule. The deviation can be classified into three categorizes, depending on the blend composition dependence of the viscoelastic function. These categories are (i) positive derivation, (ii) negative deviation, and (iii) positive-negative deviation depending on whether the deviation from the log-additivity rule is positive, negative, or both in different composition regions.

According to the plot shown in Figure 12, it can be seen that the blends show similar value of complex viscosity at all frequencies in our experiment. The complex viscosity, η^* (ω) of these blends tend to decrease as increasing PTT content and it provide the negative deviation from the log-additivity rule. Implying that this is the typical for miscible polymer blends

4. CONCLUSIONS

Miscibility of PTT/PET blends in amorphous phase can be determined by a single glass-transition temperature varies with composition. The dependence of T_g on the blend compositions were predicted by the Fox and Gordon-Taylor 's equation. The result shown that Gordon-Taylor 's equation provides a satisfactory description to the experimental data better than that of Fox's equation.

The crystallization behavior of PTT/PET blends was studied using the cold crystallization temperature (T_{cc}) and the crystallization temperature from melting state (T_c). It was found that the presence of PTT content increases or enhances the blends to crystallize from the glassy state. However the crystallization from melting

state was retarded by the presence of the minor component in the blends. These PTT/PET blends show double melting temperatures at 25-60% PTT contents, with increasing the minor component in the blends, the lowering in the apparent melting temperature was observed.

WAXD study shows that no new peak occurs in diffraction pattern, implying that PTT and PET crystallize separately and there is no co-crystallite in the blends under our experimental condition. The degree of crystallinity of each component in the blends decreases as increasing the other component. In addition, the blend of 50PTT/50PET shows the lowest total degree of crystallinity. The tensile strength of these blends was found to increase as increasing the minor component up to 40%. The 50PTT/50PET blend shows the lowest tensile strength.

Lastly, for the steady rate sweep test shown that these blends behave as a shear-thinning fluid at low shear rate studied. In case of dynamic measurements, the complex viscosity, η^* (ω) of these blends decrease as increasing PTT content and it provide the negative deviation from the log-additivity rule. Implying that this is the typical for miscible polymer blends

5. ACKNOWLEDGMENTS

The authors wish to thank Dr. Hoe H. Chuah and his co-workers of Shell Chemical Company (USA) Ltd. for supply of PTT and for their kind assistance on molecular weight measurements on all of the polyester resins received, Dr. Gi-Dae Choi and Soo-Min Lee of LG Chem (Korea) Ltd. for supply of PBT, and Assoc. Prof. Anuvat Sirivat for providing technical knowledge and helpful suggestion. PS acknowledges a grant provided by Chulalongkorn University through the Development Grants for New Faculty/Researchers. Partial in-kind support from the Petroleum and Petrochemical College is also greatly acknowledged.

REFERENCES

[1] Chuah H, in John Scheirs and Timothy Long ed. "Modern Polyester", John Wiley.

[2] Escala A and Stein RS, Advances in Chemistry Series 1979, 176, 455.

[3] Mishra SP and Deopura BL, Polymer Communications 1985, 26, 5.

[4] Mishra SP and Deopura BL, J Appl Polym Sci 1987, 33, 759.

[5] Avramov I and Avramova N, J Macromol Sci 1991, B30, 335.

[6] Avramova N, Polymer 1995, 36, 801.

[7] Shonaike GO, Euro Polym J 1992, 28, 777.

[8] Yu Y and Choi KJ, Polym Engng Sci 1997, 37, 91.

[9] Lee SS, Kim J, Park M, Lim S, and Chul RC, J Polym Sci-Polym Phys 2001, 39, 2589

[10] Reinsch VE and Rebenfeld L, J Appl Polym Sci 1996, 59, 1913.

[11] Reinsch, VE and Rebenfeld L, J Appl Polym Sci 1996, 59, 1929.

[12] Chen HL, Macromolecules 1995, 28, 2845.

[13] Jang J, Sim K, Polymer 1997, 38, 4043.

[14] Huang JM, and Chang FC, J Appl Polym Sci 2002, 84, 850.

[15] Couchman PR, Karasz FE, Macromolecules 1978, 11, 117.

[16] Gordon M, Taylor JS, J Appl Chem 1952, 2, 493.

[17] Utracki LA, Adv Polym Technol 1985, 5, 33.

[18] Fox TG, Bull Am Phys Soc 1956, 2, 123.

[19] Merfeld GD and Pual DR, in Pual DR and Bucknall CB, "Polymer Blends," Vol 1, John Wiley & Sons, New York, 1999, pp 81.

[20] Stein RS, Khambatta FB, Warner FP, Russell T, Escala A, and Balizer E, J Polym Sci, Polym Symp 1978, 63, 313.

[21] Wang B, Li YC, Hanzlicek J, Cheng SZD, Gail PH, Grebowicz J, and Ho RM, Polymer 2001, 42, 7171.

[22] Wang ZG, Hsiao BS, Fu BX, Lui L, Yeh F, Sauer BB, Chang H, and Schultz JM, Polymer 2000, 41, 1791.

[23] Desborough IJ, Hall IH, and Neisser JZ, Polymer 1979, 20, 419

[24] Yishikawa K, Molnar A, and Eisenberg A, Polym Eng Sci 1994, 34, 1056.

CAPTION OF FIGURES

Figure 1 The plots of the 10% weight loss temperature (T_{onset}) and the 50% weight loss temperature (T_{50}) of PTT/PET blends as a function of PTT content.

Figure 2 (a) DSC cold crystallization and melting thermograms for quenched PTT, PET, and PTT/PET blend samples recorded during heating at $10^{o}C\ min^{-1}$, and (b) DSC melt crystallization exotherms for PTT, PET, and PTT/PET blend samples recorded during subsequent cooling at $10^{o}C\ min^{-1}$.

Figure 3 Observed glass transition temperature T_g for quenched PTT, PET, and PTT/PET blend samples as a function of blend composition.

Figure 4 Cold crystallization (peak) temperature T_{cc} for quenched PTT, PET, and PTT/PET blend samples as a function of blend composition.

Figure 5 Melt crystallization (peak) temperature T_c for quenched PTT, PET, and PTT/PET blend samples as a function of blend composition.

Figure 6 Melting (peak) temperature T_m characterizing the melting of PTT and/or PET crystallites (after cold crystallization process) for quenched PTT, PET, and PTT/PET blend samples as a function of blend composition.

Figure 7 Wide-angle X-ray diffractograms for PTT, PET, and PTT/PET blend samples after non-isothermally crystallized from the molten state in DSC cell at a cooling rate of $10^{o}C{\cdot}min^{-1}$.

Figure 8 Apparent degree of crystallinity for PTT and PET components for both pure and blend samples as a function of blend composition.

Figure 9 Tensile strength of PTT, PET, and blends as a function of PTT content.

Figure 10 The steady shear viscosity η measured at $260^{o}C$ for PTT, PET, and PTT/PET blend samples as a function of shear rate.

Figure 11 The zero shear viscosity values for PTT, PET and PTT/PET blend samples as a function of blend composition.

Figure 12 The plot of complex viscosity (η^*) at constant frequency as a function of blend composition.

Table 1 Characteristic X-ray peaks and the total degree of crystallinity of PTT, PET, and blends

Blend composition	Characteristic X-ray peaks (2θ)														Degree of crystallinity
PET	-	16.08	-	17.5	-	21.6	-	22.8	-	-	25.9	-	28.1	32.6	22.3
10PTT/90PET	-	16.1	-	17.6	-	21.5	-	22.7	-	-	25.9	-	27.8	32.5	23.2
25PTT/75PET	-	16.16	-	17.5	-	21.4	-	22.7	-	-	25.9	-	27.9	32.4	19.4
40PTT/60PET	15.5	16.16	-	17.5	-	21.6	-	22.7	23.4	24.5	25.8	-	28.0	32.7	14.5
50PTT/50PET	15.7	-	16.9	17.3	19.7	21.6	-	22.6	23.9	24.8	26.2	27.6	-	32.9	13.7
60PTT/40PET	15.4	-	16.7	17.4	19.8	-	21.8	-	23.6	24.6	26.0	27.2	-	32.7	20.1
75PTT/25PET	15.4	-	16.9	-	19.5	-	21.7	-	23.6	24.7	-	27.5	-	-	22.4
90PTT/10PET	15.3	-	16.8	-	19.3	-	21.6	-	23.4	24.6	-	27.6	-	-	23.8
PTT	15.3	-	16.8	-	19.4	-	21.7	-	23.6	24.6	-	27.3	-	-	24.8

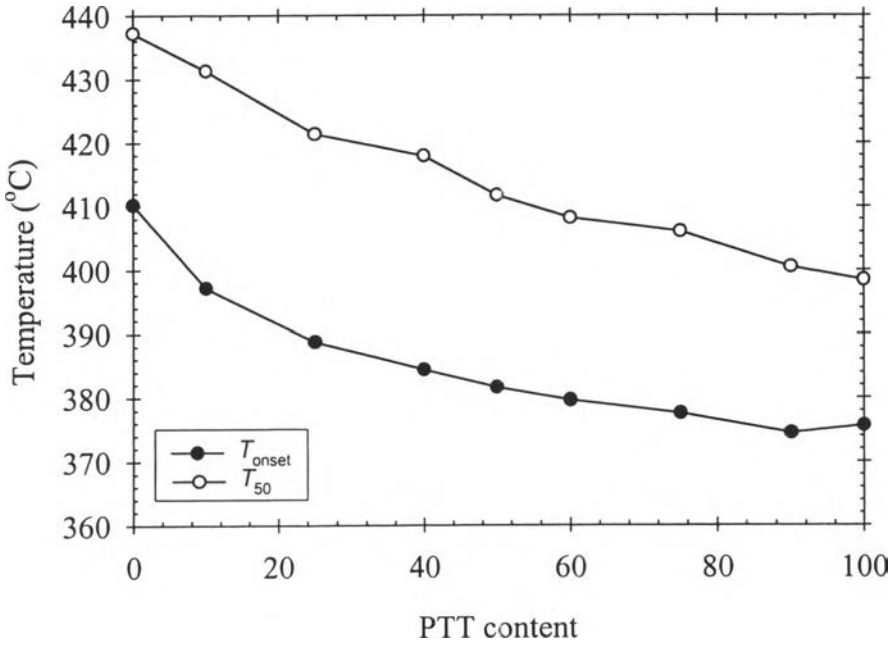
440
430
420
410
400
390
380
370
360
Temperature (°C)
0
20
40
60
80
100
PTT content
T_{onset}
T_{50}

Figure 1

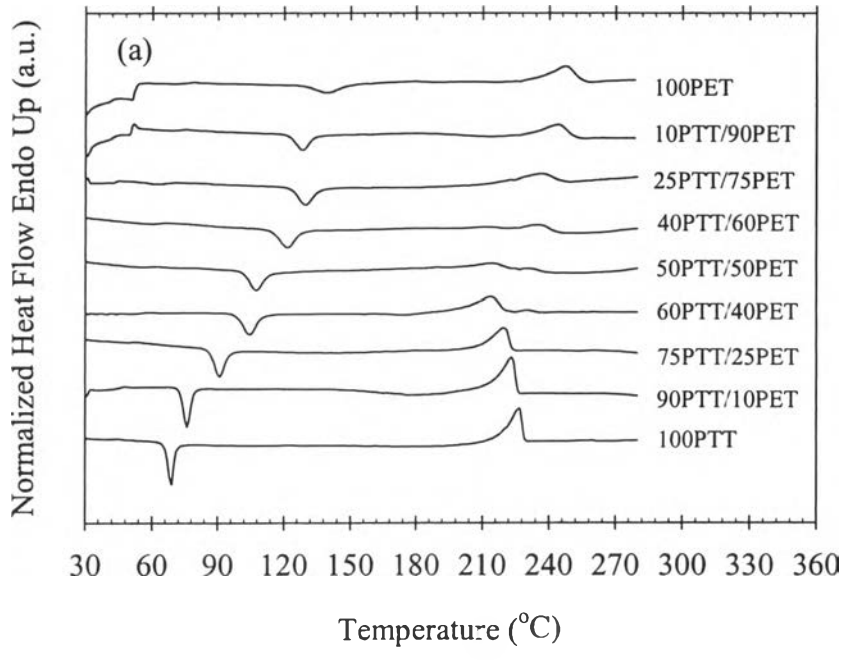
(a)
100PET
10PTT/90PET
25PTT/75PET
40PTT/60PET
50PTT/50PET
60PTT/40PET
75PTT/25PET
90PTT/10PET
100PTT
Normalized Heat Flow Endo Up (a.u.)
30 60 90 120 150 180 210 240 270 300 330 360
Temperature (°C)

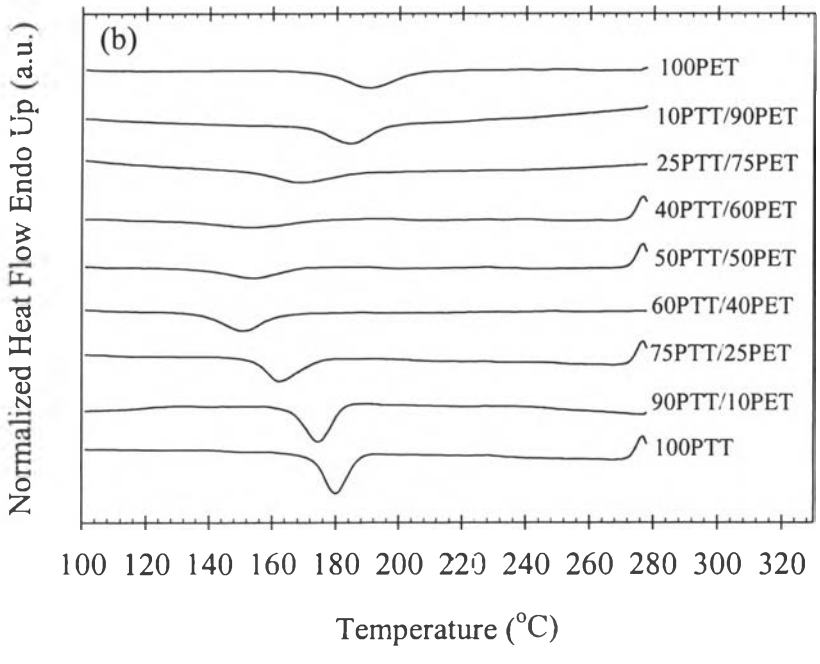
(b)
100PET
10PTT/90PET
25PTT/75PET
40PTT/60PET
50PTT/50PET
60PTT/40PET
75PTT/25PET
90PTT/10PET
100PTT
Normalized Heat Flow Endo Up (a.u.)
100 120 140 160 180 200 220 240 260 280 300 320
Temperature (°C)

Figure 2

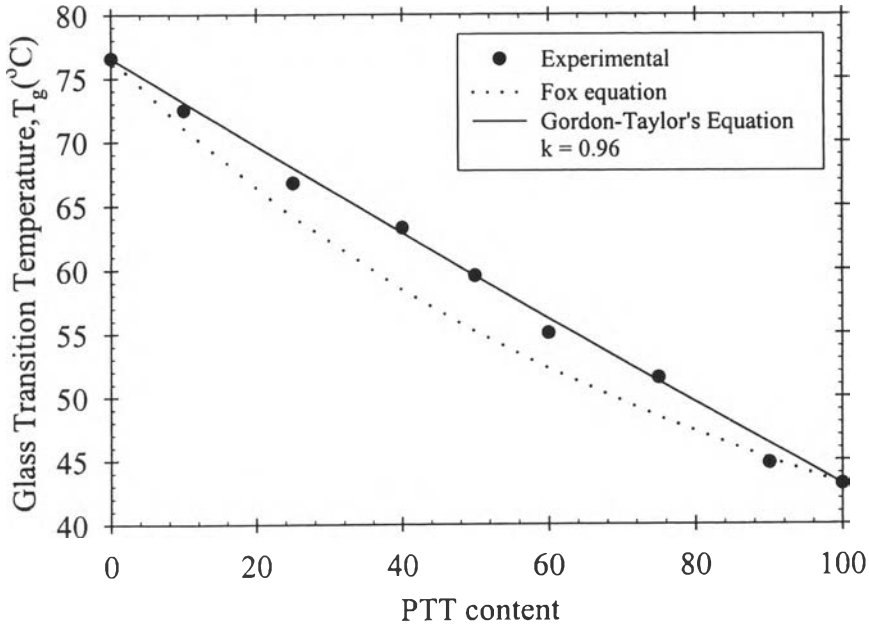
Glass Transition Temperature, T_g(°C)
80
75
70
65
60
55
50
45
40
0
20
40
60
80
100
PTT content
Experimental
Fox equation
Gordon-Taylor's Equation
k = 0.96

Figure 3

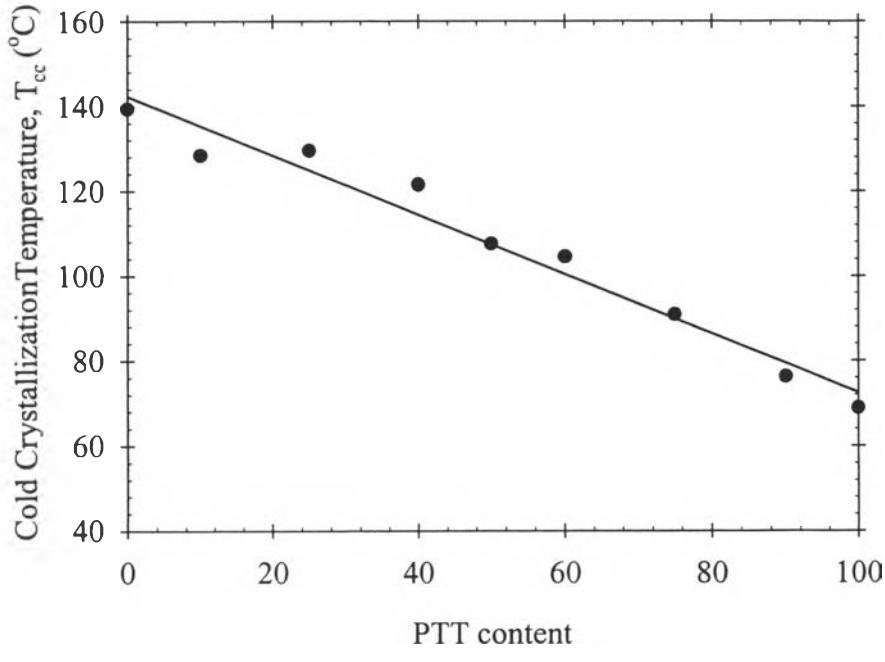
Cold CrystallizationTemperature, T_{cc} (°C)
160
140
120
100
80
60
40
0
20
40
60
80
100
PTT content

Figure 4

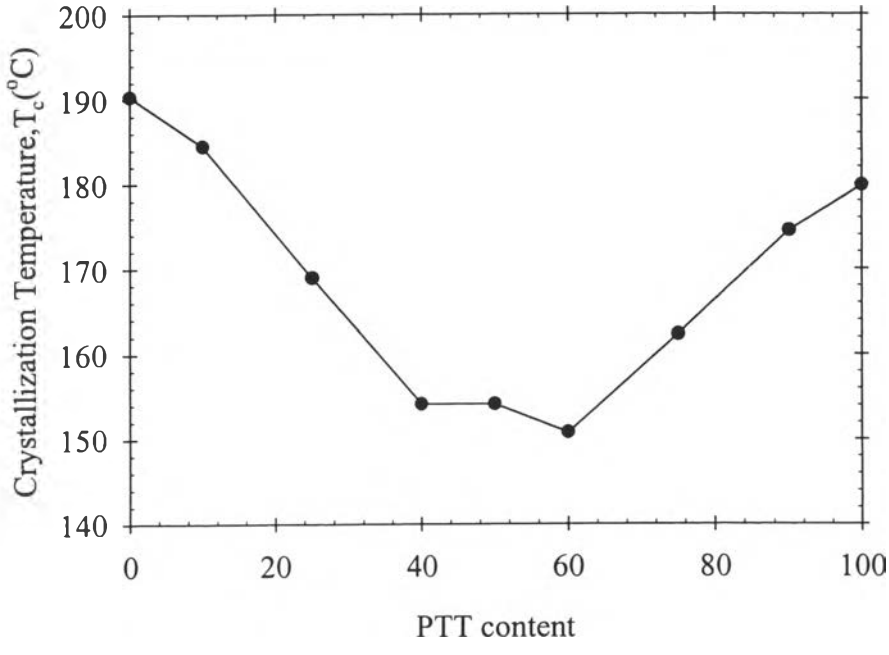
Crystallization Temperature, T_c(°C)
200
190
180
170
160
150
140
0
20
40
60
80
100
PTT content

Figure 5

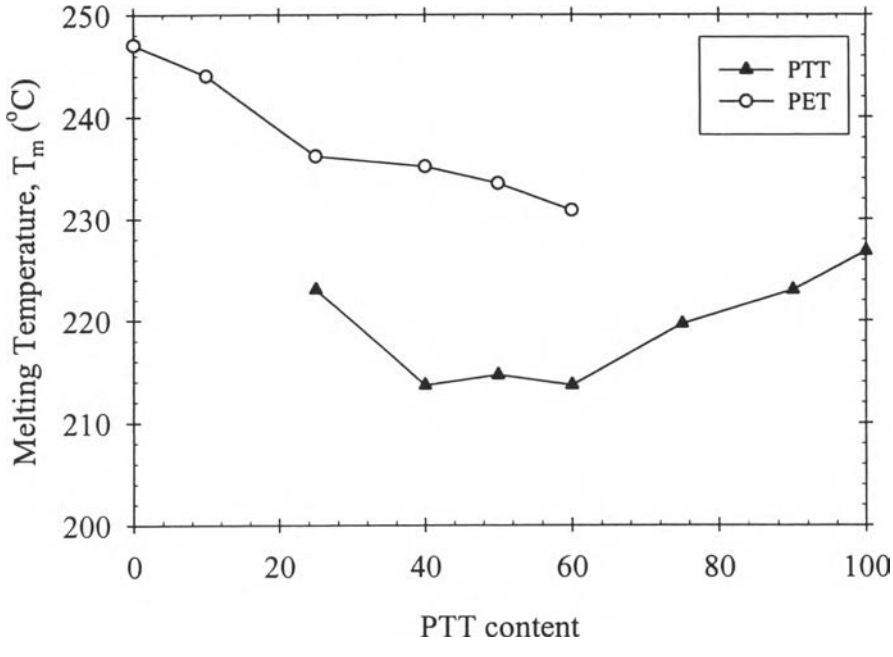
250
240
230
220
210
200
Melting Temperature, T_m (°C)
0
20
40
60
80
100
PTT content
PTT
PET

Figure 6

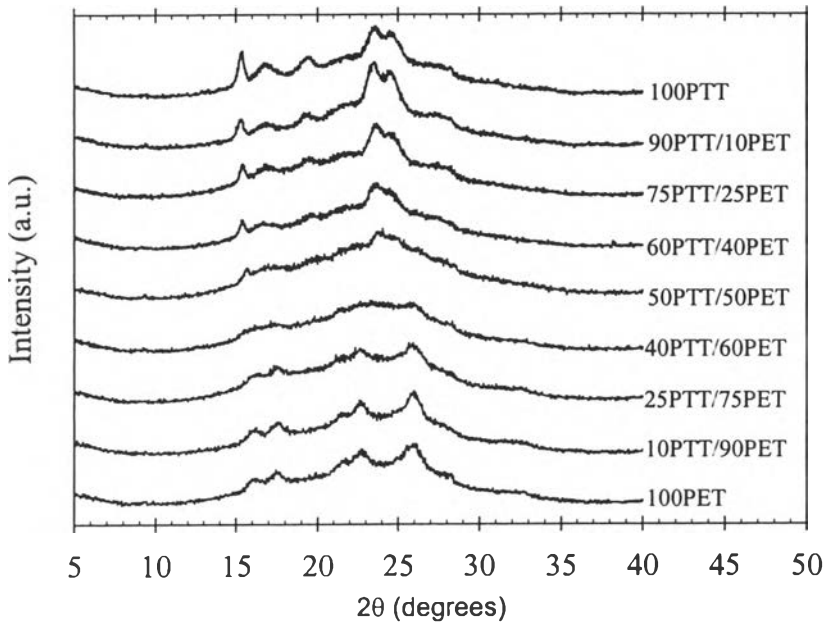
Intensity (a.u.)
100PTT
90PTT/10PET
75PTT/25PET
60PTT/40PET
50PTT/50PET
40PTT/60PET
25PTT/75PET
10PTT/90PET
100PET
5
10
15
20
25
30
35
40
45
50
2θ (degrees)

Figure 7

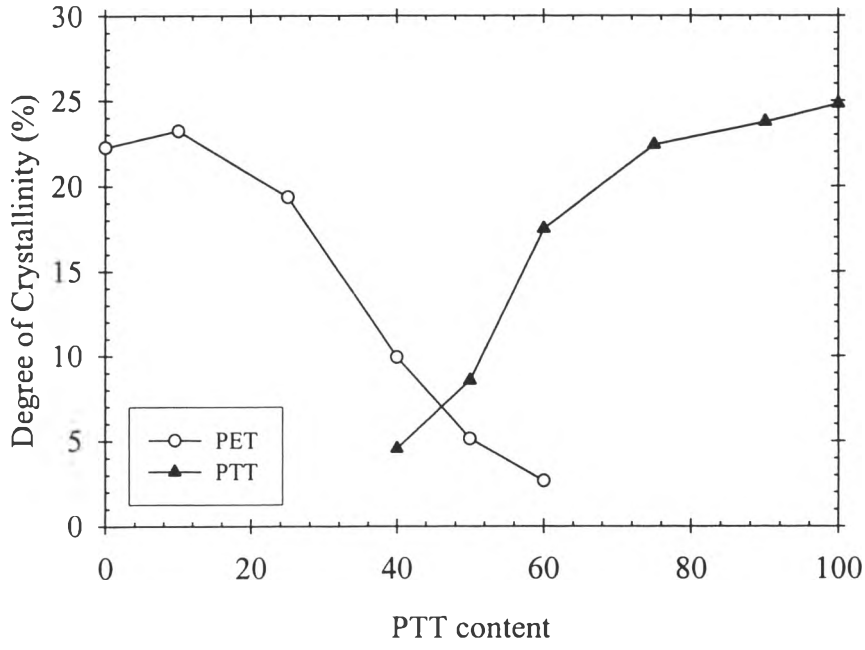
Degree of Crystallinity (%)
30
25
20
15
10
5
0
0
20
40
60
80
100
PTT content
PET
PTT

Figure 8

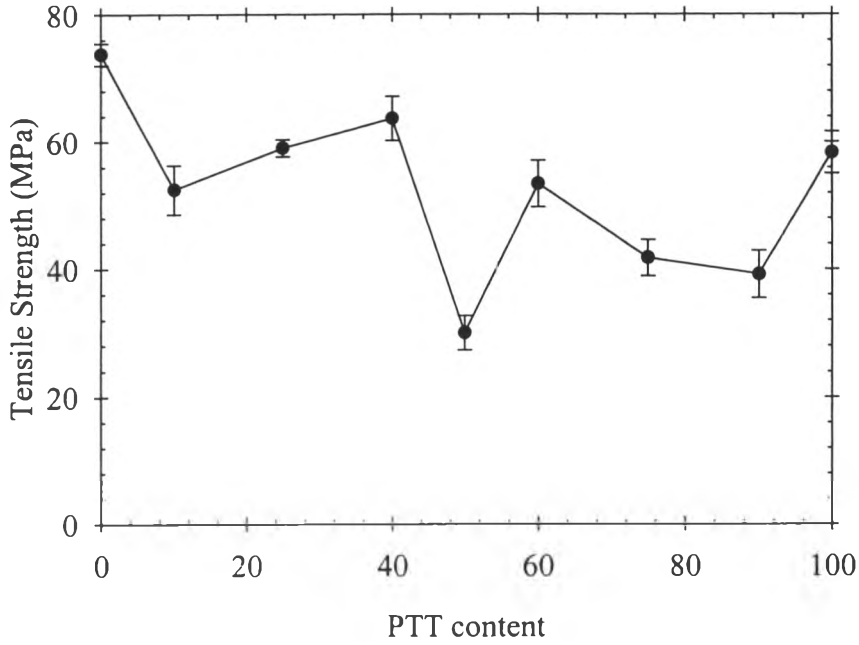

Figure 9

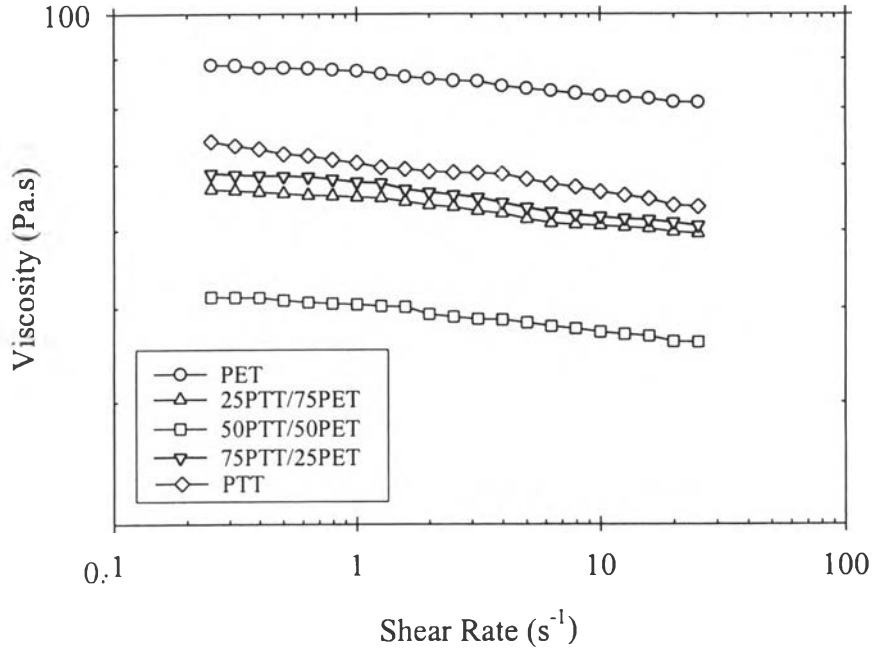
100
Viscosity (Pa.s)
PET
25PTT/75PET
50PTT/50PET
75PTT/25PET
PTT
0.1
1
10
100
Shear Rate (s-1)

Figure 10

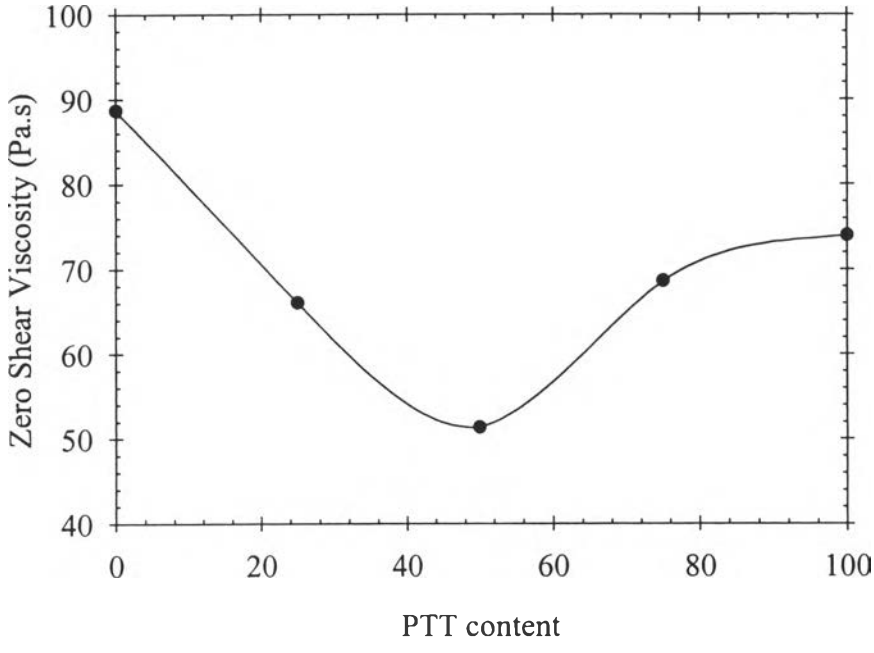
Zero Shear Viscosity (Pa.s)
100
90
80
70
60
50
40
0
20
40
60
80
100
PTT content

Figure 11

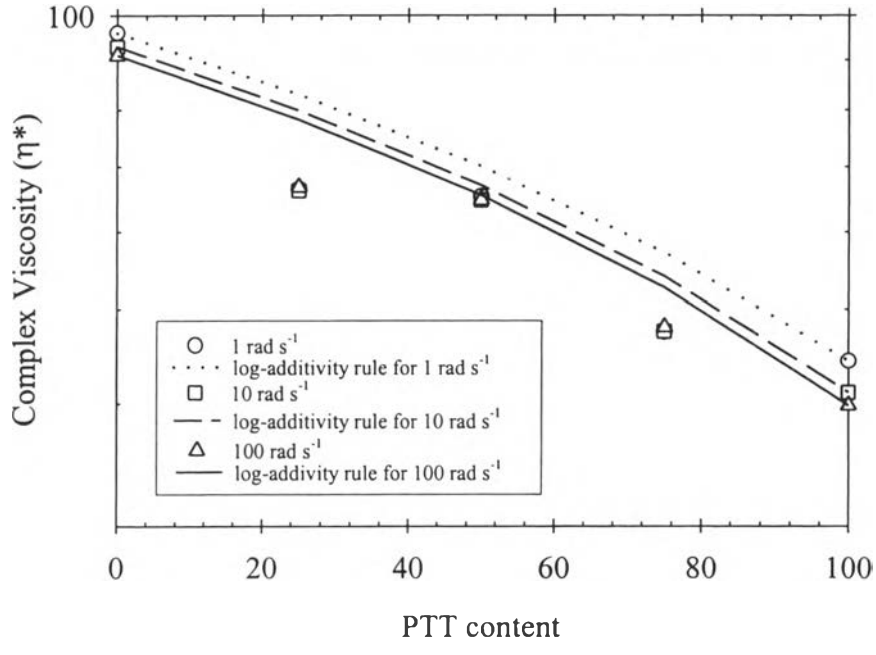
100
Complex Viscosity (η*)
1 rad s-1
log-additivity rule for 1 rad s-1
10 rad s-1
log-additivity rule for 10 rad s-1
100 rad s-1
log-addivity rule for 100 rad s-1
0
20
40
60
80
100
PTT content

Figure 12